EFFECTS OF DIFFERENT COATINGS ON THERMAL STRESS OF SOLAR PARABOLIC TROUGH COLLECTOR ABSORBER IN DIRECT STEAM GENERATION SYSTEMS

Farhad Razmmand* [*], *Ramin Mehdipour* [*1]

[*] Department of Mechanical Engineering, Tafresh University, Markazi, Iran

Corresponding author; mehdipour@tafreshu.ac.ir

Today, solar parabolic trough collectors are the most appropriate technologies in solar power generation due to higher efficiencies in comparison with other collector types. In this paper, a numerical heat transfer model is considered, for simulation of this equipment. The inlet heat flux to the absorber is calculated to be considered as a boundary condition for the external surface of the absorber. Temperature distribution on the absorber is obtained, by the aid of energy equilibrium modeling. Thereupon, thermal and pressure stress at absorber are analyzed in the model by thermal results and finite element methods. In this study, the direct steam generation system is used as the basis for the work. High thermal stress is a defect in direct steam generation systems. In this research thermal performance is improved and stress tolerance can be increased by using the coating on absorber surface. At the end, the most suitable coating is introduced among the variety of considered coatings types.

Key Words*: Solar power plant; Parabolic trough collector; Direct steam generation system; Heat transfer analysis; Thermal stress analysis; Coating*

1. Introduction

In direct steam generation solar power plants, water is being used instead of oil as a fluid which in some cases leads to some fractures in the absorber. It should be noted that fractures mostly occurs in the part wherein the fluid has a boiling regime. The cause of this problem is related to extreme changes in the thermal fluid in a short distance. There are several ways to strengthen and lowering the thermal stress in the absorber from those proper coating can be noted [1]. In choosing the coating material economic factors should be considered in addition to its specifics related to its application [2].

Concentrated solar power plants are one of most applied production procedures by renewable energy. Amongst, linear parabolic trough collectors are the most economical technology for absorbing solar energy [3]. Predicting thermal distribution in the solid material under non-uniform thermal source is one of attracting subjects in the context of designing the solar absorber. To estimate temperature gradient level and non-uniform effective thermal stress, extensive investigations with three perspectives are implemented as below:

1) Studying transient effects of the non-uniform thermal source on a pipe [4] 2) Studying effects of thermal fluid specifications, pipe design and sun beams emitting concentration over the concentrating complex [5] 3) Experimental/ numerical simulations to control thermal stresses [4-6]. Most of the accomplished numerical studies in the literature [7-10] are devoted to the analysis of heat transfer in linear parabolic trough collectors. The fluid flow at the entrance of the considered system is single-phase while by absorbing heat, some bubbles form and two-phase boiling flow are obtained.

Effects of some important parameters as temperature and mass flow rate of the inlet water, tube transmittance and the properties of the absorber surface, on the collector's energy and exergy efficiency, has been investigated by [11-14]. Zhu et al. [15] studied the performances of organic Rankine cycle using organic fluids. Their aim was to recover heat from renewable or waste energy sources.

Solar collectors usually are installed in open areas which are faced with high winds. Hachicha et al. [5] investigated computational fluid dynamics of wind flow around a linear parabolic trough concentrator under real working conditions.

In electricity generating power plants by solar energy, the geometry of devices such as absorber are of great importance. To achieve certain ranges of geometrical parameters with optimized quality, Cheng et al. [16] theoretically analyzed the relations between geometrical parameters of the invertor part and system`s focal form. As well, Akbari et al. [17] have performed a theoretical study to discuss concentration ratio, flux density, temperature distribution and thermal expansions effects over designing conditions. Thermal stress caused by boiling is studied by considering the thermal profile of boiling at the inner surface of the pipe [18, 19].

In the present study, the direct steam generation system is considered as the power generation system of the solar plants. Water is used as the working fluid which is proved to show better performance than oil [20]. The fluid flow from the entrance to the outlet experiences three different regimes which are comprehensively modeled. Fluid at the pipe inlet is single phase while by flowing through the pipe and absorbing heat the temperature rises to the boiling point and some bubbles forms. At this stage, since the fluid bulk temperature is still below the saturation temperature, the formed bubbles may condense after detaching the pipe wall. This regime is called sub-cooled flow regime and may last until the bulk temperature reaches saturation condition. Then the fluid is in the two-phase boiling regime. Due to high-temperature gradient throughout the absorber, considerable thermal stress at the absorber surface results. To reduce these effects and prevent fractures due to thermal stresses, three kinds of coatings, namely titanium carbide; black chromium; and nickel, are evaluated. Common roller shaping is applied for coating the pipe. To demonstrate the connection between the coating and the pipe in the modeling the sign "Tie" is used in the figures. It will be shown that tangential thermal stress distribution in the absorber coated with titanium carbide is lower than two other coats.

2. Simulation of a linear parabolic receiver and governing approach

The general modeling approach in the present study is the energy balance of the heat collector element. The equation generally consists of direct sun's irradiance, the optical loss of the parabolic mirror and the heat collector element, heat losses of the heat collector element as well as fluxes and heats existing in heat transfer fluid.

During a day, the Sun's irradiance on the collector and mirror complex first gets to the parabolic mirror and reflects off it and then gets concentrated in the heat collector element placed in the focal distance. On the way, a small amount of the energy with the quantity of $\dot{q}_{g,s.rad}$ is absorbed by glass the and the rest of the energy with the quantity of $\dot{q}_{g,cond}$ passes the glass after passing the width of the glass wall with heat transfer by conduction and gets to the absorber by radiation heat transfer. The quantity of the radiated energy is equated to $\dot{q}_{a,s.rad}$. Some part of the absorbed energy after passing the absorber wall by conduction heat transfer with the quantity of $\dot{q}_{a,cond}$, by convection heat transfer with the quantity of $\dot{q}_{a-f,conv}$ is transferred to heat transfer fluid and in this step the remain returns to the glass by free convention heat transfer ($\dot{q}_{a-g,conv}$) and radiation heat transfer ($\dot{q}_{a-f,rad}$). Finally the sum of thermal energies arrived the glass by process of convection heat transfer ($\dot{q}_{g-e,conv}$) is transferred to the environment. The heat transfer circuit of these steps is in Fig. 1. These steps can be seen in Fig. 2.

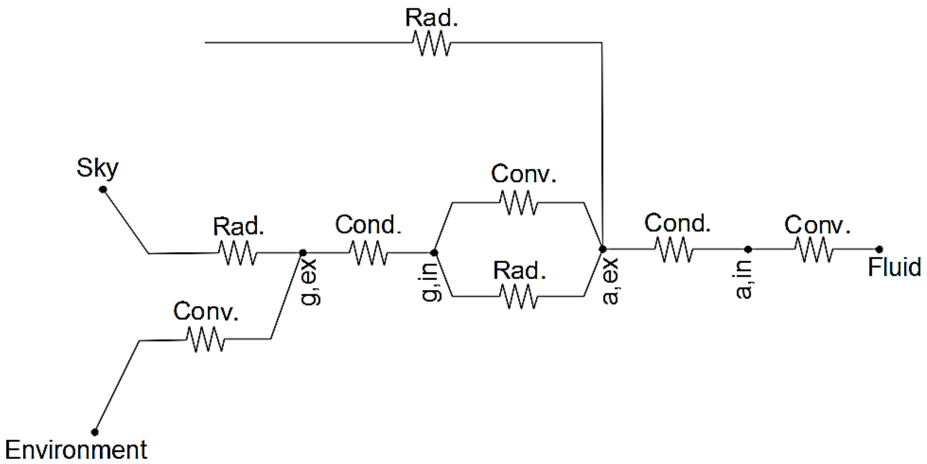

Fig. 1. Heat transfer circuit

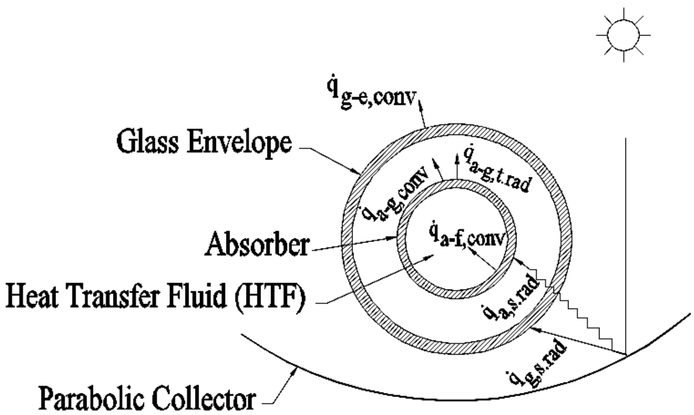

Fig. 2. Heat transfer model at the cross section of the heat collector [1]

Each heat transfer process of the absorber, as well as its related equation, will be discussed in the following sections.

3. Radiation heat transfer over the glass and on the surface of absorber and Conduction heat transfer through the glass

As explained before, after reaching parabolic mirror, some sunlight beams are absorbed to the mirror and the rest goes to the glass and absorber complex placed at a focal distance. The quantity of the beams radiated to the glass can be achieved as the following equations, [18]

$$\dot{q}_{g,s.rad} = \frac{2(\dot{q}_{sun,g}\alpha_g)}{3} \tag{1}$$

$$\dot{q}_{sun,g} = I_{sun}\beta w C r_g \tag{2}$$

After reaching the thermal energy to the glass by radiation, it passes through the glass wall by conduction heat transfer (Equation 3) [18]:

$$\dot{q}_{g,cond} = \frac{2\pi k_g (T_{g,ex} - T_{g,in})}{\ln\left(\frac{D_{g,ex}}{D_{g,in}}\right)} \tag{3}$$

At this stage, a fracture of heat reached to the glass is absorbed according to absorption factor of the glass and transfers to the absorber after passing the glass wall as equation 4, by considering transmission ratio of glass. The amount of this thermal energy can be calculated as below:

$$\dot{q}_{a,s.rad} = \frac{2(\dot{q}_{sun,a}\gamma\alpha_a)}{3} \tag{4}$$

$$\dot{q}_{sun,a} = I_{sun}\beta w C r_a \tag{5}$$

4. Conduction heat flux in the absorber and convection heat flux from the pipe to the fluid

At this section, the heat is absorbed by the absorber and by conduction heat transfer process passes through the absorber`s wall. This heat transfer is explained by equation (6) [18]:

$$\dot{q}_{a,cond} = \frac{2\pi k_a \left(T_{a,ex} - T_{a,in}\right)}{\ln\left(\frac{D_{a,ex}}{D_{a,in}}\right)} \tag{6}$$

Inside the pipe, the fluid is limited by the absorber`s wall as an internal flow. So the boundary layer can`t develop freely without contact with surfaces [18]. After the heat passes the absorber`s wall by conduction, the heat is transferred to the fluid inside the pipe. This transfer is of internal convection type. The following equations describe the above-mentioned heat transfer [1, 18]:

$$\dot{q}_{a-f,conv} = h_f \pi D_{a,in}\left(T_{a,in} - T_m\right) \tag{7}$$

$$Nu_f = 0.023 Re^{0.8} Pr^{0.4} \tag{8}$$

5. Fluid energy equations

In addition to what explained before about convection heat transfer from the absorber to the fluid, because the flow is totally surrounded by the absorber, average temperature changes and the relation between convection heat $\dot{q}_{a-f,conv}$ and temperature difference between input and output can be calculated by energy balance, [18].

Fluid is flowing with constant flow rate $\dot{m}$ inside the absorber and convection heat transfer occurs between its surface and the fluid. The below relations show the fluid element`s energy balance. [11, 18]

$$\dot{q}_{a-f,conv} = \frac{q_{f,conv}}{l} \tag{9}$$

$$q_{f,conv} = \dot{m} C_p (T_{out} - T_{in}) \tag{10}$$

6. Convection and radiation heat flux between the absorber and the glass

After reaching the absorber, according to its absorption factor, some of the thermal energy is absorbed by the pipe and by two processes of conduction and convection heat transfer passes the wall and transfers to the fluid. After absorbing this amount of heat, some is reflected in the glass by two processes of free convection and radiation heat transfer according to reflection ratio of the absorber (pipe).

For the condition that is considered in this study, heat is transferred from the pipe to the glass, so the pipe temperature is more than the glass temperature [1, 18]:

$$\dot{q}_{a-g,conv} = h_c \pi D_{a,ex} \left(T_{g,in} - T_{a,ex}\right) \tag{11}$$

$$h_c = \frac{2k_{eff}}{D_{a,ex} \ln\left(D_{g,in}/D_{g,ex}\right)} \tag{12}$$

As explained above, after absorbing the heat in the absorber the rest of the thermal energy is transferred to the glass by two processes of heat transfer. In this section, we explain a little about the radiation heat transfer from the absorber to the glass and note the relevant relations as well. Absorber and glass surfaces are considered diffuse gray body, emitter, and reflector. As well, the glass is considered as opaque material toward thermal radiation, [18]. The following equation explains this part of heat transfer,

$$\dot{q}_{a-g,rad} = F_{rad} \sigma \pi D_{a,ex} \left({T_{g,in}}^4 - {T_{a,ex}}^4\right) \tag{13}$$

7. Convection heat flux from the glass to the surrounding environment

After two processes of heat transfer from the absorber to the glass, thermal energy passes through the glass and by convection heat transfer is transferred to the environment. At this step generally, there are free and forced convection simultaneously. In the primary modeling a calm atmosphere without wind blowing is considered, eventually, the heat flow is considered to be free convection. Relevant relations for modeling this part of heat transfer are [1, 14, 18]:

$$\dot{q}_{g-e,conv} = h_e \pi D_{g,ex} \left(T_{g,ex} - T_{amb}\right) \tag{14}$$

$$Nu_e = \left\{0.6 + \frac{0.387 Ra^{1/6}}{\left(1 + (0.559/Pr_e)^{9/16}\right)^{8/27}}\right\}^2 \tag{15}$$

8. Energy balance equations

First law of thermodynamics is applied as a useful tool for many heat transfer problems. In the present model two control volumes, control volume of the glass and control volume of the absorber can be considered. Relations 16 and 17 respectively are the relations of energy conservation of the control volumes considered for the glass and the absorber.

$$\dot{q}_{g,s.rad} + \dot{q}_{a-g,conv} + \dot{q}_{a-g,rad} - \dot{q}_{g-e,conv} = 0 \tag{16}$$

$$\dot{q}_{a,s.rad} - \dot{q}_{a-f,conv} - \dot{q}_{a-g,conv} - \dot{q}_{a-g,rad} = 0 \tag{17}$$

The energy balance on the interface of the glass and the absorber can be written as:

$$\dot{q}_{g,cond} + \dot{q}_{a-g,conv} + \dot{q}_{a-g,rad} = 0 \tag{18}$$

$$\dot{q}_{a,cond} - \dot{q}_{a-f,conv} = 0 \tag{19}$$

9. Stress equations

Thermal stress equations governing the absorber are [6]:

$$\sigma_z = \frac{E.\beta_c}{(1-\nu).r^2}\left[\frac{2}{{r_{out}}^2 - {r_{in}}^2}.\int_{r_{in}}^{r_{out}} T(r).r.dr - T(r)\right] \tag{20}$$

$$\sigma_r = \frac{E.\beta_c}{(1-\nu).r^2}\left[\frac{r^2 - {r_{in}}^2}{{r_{out}}^2 - {r_{in}}^2}.\int_{r_{in}}^{r_{out}} T(r).r.dr - \int_{r_{in}}^{r} T(r).r.dr\right] \tag{21}$$

$$\sigma_\theta = \frac{E.\beta_c}{(1-\nu).r^2}\left[\frac{r^2 - {r_{in}}^2}{{r_{out}}^2 - {r_{in}}^2}.\int_{r_{in}}^{r_{out}} T(r).r.dr + \int_{r_{in}}^{r} T(r).r.dr - (T(r).r^2)\right] \tag{22}$$

10. Solution algorithm

The numerical solution is performed by applying one-dimensional element under stable conditions. Energy balance equations (equations 16 to 19) is solved in a system of nonlinear algebraic equations as for how the relations including temperatures and fluxes are added to the system as well and by a repeating process, with solving a system of 13 equations with 13 unknowns using coding, the unknowns are calculated [1]. In continuation, the internal temperature of the surface of the absorber is calculated, then by this actual approach, the temperature for higher control values is calculated. The system of equations performs this process by a direct linear solution and iteration method in the longitudinal direction of the pipe [1]. The calculation accuracy has been considered to be equal to 0.001 for stability and calculation is converged for each element after 17 iterations.

Therefore, the general solution algorithm is divided into two main parts: 1) calculating the distribution of the concentrated heat transfer from the sun to the mirror and then to the glass and the absorber by coding in order to calculation of temperature distribution for external and internal surface of absorber 2) Analyzing the thermal stress by consider the temperature distribution and Constraints as boundary conditions in the software of stress simulation

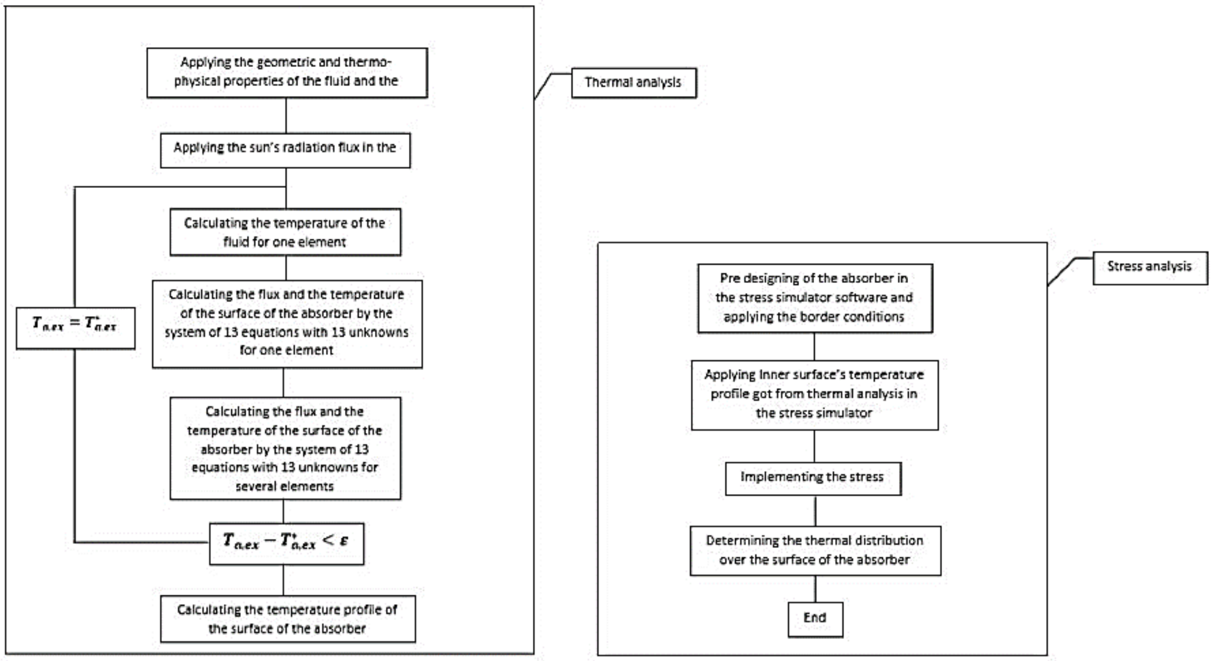

Fig. 3. Solution algorithm

11. Modeling validation

The geometry of the applied model for validation based on the reference [19] is shown in Fig. 4.

In this study, the applied fluid is synthetic oil. The thermophysical properties of this fluid, as well as the parameters of the absorber, are shown in tables 1 and 2.

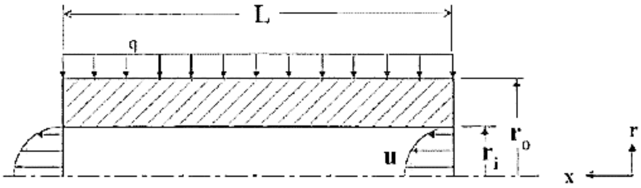

Fig. 4. Considered geometry for thermal modeling and stress analysis in the absorber [19]

Table1. Parameters of the geometry of the glass and the absorber [1]

Parameter	Value	Parameter	Value
Receiver length	7.8 (m)	Glass internal diameter	0.109 (m)
Collector aperture	5 (m)	Glass external diameter	0.115 (m)
Focal distance	1.84 (m)	Receiver absorbance	0.96
Absorber internal diameter	0.066 (m)	Glass transmittance	0.95
Absorber external diameter	0.070 (m)	Parabola specular reflectance	0.93

Table 2. Laboratory parameters used in the analysis according to [1]

Parameter	Value	Unit	Parameter	Value	Unit
Selective coating	Black chrome		Input temperature	375.35	(K)
Thermal conductivity for selective coating	67	$(\frac{W}{m.K})$	Selective fluid	Synthetic oil	
Selective absorber	Ferritic Steel (P-22)		Gravity of fluid	709	$(\frac{kg}{m^3})$
Thermal conductivity for selective absorber	33	$(\frac{W}{m.K})$	Thermal conductivity of fluid	0.078	$(\frac{W}{m.K})$
Incident solar irradiation	933.7	$(\frac{W}{m^2})$	Viscosity of fluid	1.52 E -4	$(\frac{kg}{sec.m})$
Wind speed	0.03	$(\frac{m}{s})$	Specific heat of fluid	2588	$(\frac{J}{kg.K})$
Air temperature	294.35	(K)			

As seen in Fig. 5, there is a good consistency between the obtained outlet fluid temperature with that of Ref. [1].

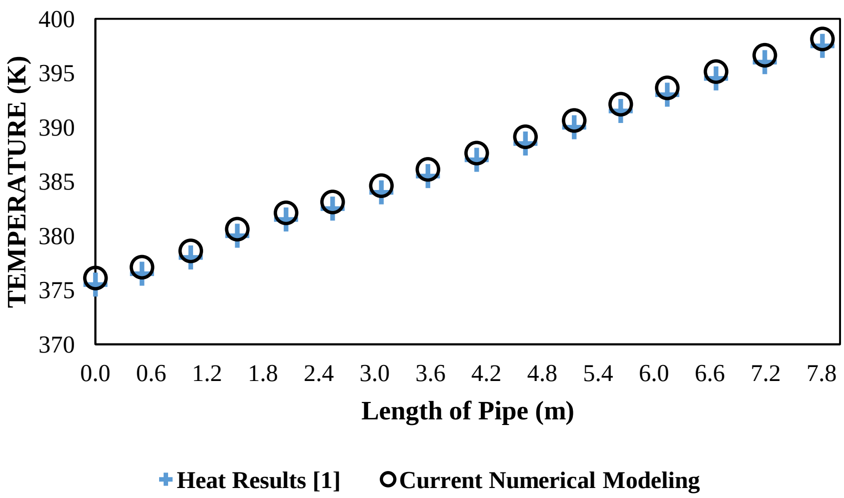

Fig. 5. Fluid temperature of the present analysis and the obtained results of [1]

About stress validation, we got aid from two different references. First results of thermal stresses in the present study are compared with that of ref. [19]. In this investigation, the properties of the absorber and the working fluid are as shown in Table 3.

Table 3. Properties of the absorber and the working fluid used in [19]

Solid		Fluid	
Absorber Type	Steel	Fluid Type	Water
Thermal conductivity ($\frac{W}{m.K}$)	43	0.597	
Thermal expansion ($\frac{1}{K}$)	0.373 E -5	-	
Modulus of elasticity (GPa)	2.1	-	
Poisson's ratio	0.3	-	
Density ($\frac{kg}{m^3}$)	-	998.23	
Specific heat ($^{J}/_{kg.K}$)	-	4181.8	
Kinematic viscosity ($^{m^2}/_{sec}$)	-	1.006 E -6	

As noted above, in the present model, thermophysical and mechanical properties of the absorber, as well as the working fluid and geometrical specifications, are set similar to Ref. [19] to have a good comparison between the results. Distribution of the thermal stress on the inner surface of the absorber, as shown in Table 4, are in good consistency with corresponding results reported in Ref. [19]. The deviation between the results is about 5%.

Table 4. Numerical comparison of thermal stress distribution on the inner surface of the absorber in current simulation with [19]

Pipe Length (m)	Result in [19] (MPa)	Current Simulation (MPa)
0.0	243571	255749.55
0.2	201786	211875.30
0.4	142857	149999.85
0.6	190000	199500.00
0.8	210357	220874.85
1.0	218929	229875.45

In the reference [19] external coating over the absorber is not considered. For validation of thermal stress distribution on the surface of the absorber in the boiling heat transfer with coating conditions, reference [6] was used. In table. 5 and table. 6 thermo physical and mechanical properties of the working fluid, the absorber and the coating used in this analysis can be seen. Properties in the model are set similar to what is mentioned in Ref. [6].

Table. 5. Thermo physical and mechanical properties of the absorber and the fluid

Absorber		Fluid	
Copper		Thermal Oil	Steam
Density ($^{kg}/_{m^3}$)	8930	938	586.3

Specific heat ($^J/_{kg.K}$)	386	1970	2060
Thermal conductivity ($^W/_{m.K}$)	384	0.118	0.0246
Thermal expansion coefficient ($^1/_K$)	17.1 E -006	-	-
Modulus of elasticity (GPa)	128	-	-
Poisson's ratio	0.31	-	-
Kinematic viscosity ($^{m^2}/_{sec}$)	-	15.3 E -006	1.271 E -5

Table 6. Thermo physical and mechanical properties of the coatings used in this study [18]

Coating Type	Nickel	Black Chromium	Titanium Carbide
Density ($\frac{kg}{m^3}$)	1728	7160	4938
Specific heat ($\frac{J}{kg.K}$)	8900	459.8	522
Thermal conductivity ($\frac{W}{m.K}$)	12	67	110
Thermal expansion ($\frac{1}{K}$)	13.4E -6	6.2 E -6	7.7 E -6
Modulus of elasticity (GPa)	200	290	439.43
Poisson's ratio	0.31	0.03	0.188

As can be seen in Fig. 6 results of the present study are consistent with results of Ref. [6]. The deviation between the results is about 7%.

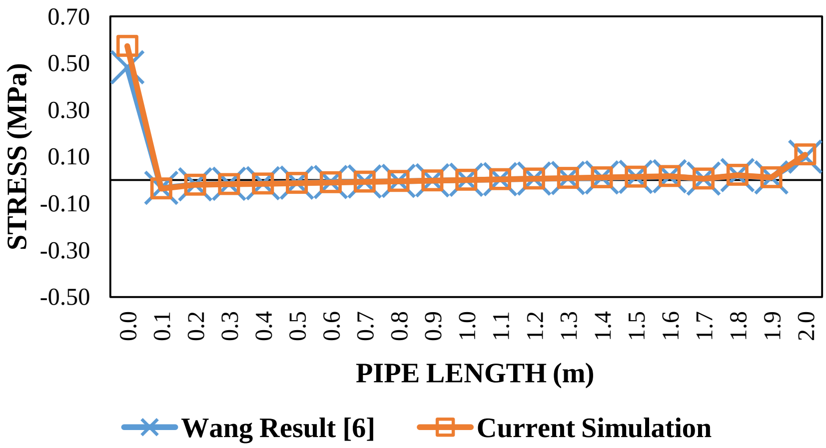

Fig. 6. Comparing radial stress distribution along the absorber in the performed analysis with the similar one in [6]

12. Boiling and superheating steps results

In this section applying three different coats of nickel, black chromium and titanium carbide in boiling and super heating steps of the model are considered, and eventually, the coating effect on the heat performance and thermal stress are studied.

At the boiling step of the model, properties of the pipe material and the fluid are as table 5. Thermo physical and mechanical properties of the primary coating which was considered for this model are as table 6. Laboratory conditions are as table 1 while the absorber length in this section is equal to 2 meters. Tangential stress distribution along the absorber which is obtained in this situation by considering three different coatings of nickel, black chrome, and titanium carbide is as Fig. 7.

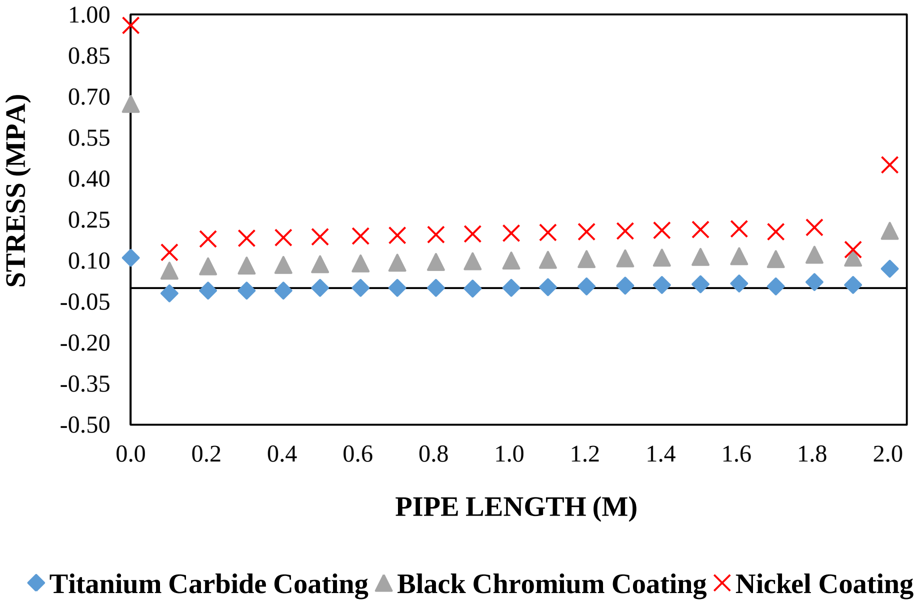

Fig. 7. Tangential stress distribution chart along the absorber at boiling step

It should be noted that for numerical analysis of the boiling part in relations mentioned at section 4, we should apply the boiling heat flux relation in numerical modeling. The relation is explained below [6, 18]:

$$\dot{q} = \mu_l h_{fg} D_{a,in} \left[\frac{g(\rho_l - \rho_v)}{\sigma}\right]^{\frac{1}{2}} \left(\frac{c_{p,l}\Delta T_e}{C_{s,f} h_{fg} {Pr_l}^{n}}\right) \tag{23}$$

$$\Delta T_e = T_s - T_{sat} \tag{24}$$

By replacing equations (23) and (24) instead of equations (7) and (8) in numerical modeling, a temperature profile results for the surface of the pipe which by applying the obtained profile in the simulation we can obtain the results of thermal stress distribution. It should be noted that due to the boiling concept and continuous heat absorption, the liquid contribution reduces and vapor phase increases. Therefore the density decreases as gas phase increases along the pipe.

As seen from Fig. 8, in nickel, black chrome and titanium carbide coatings, according to increasing the thermal conductivity coefficient for the coatings respectively, tangential thermal stress distribution decreases with the same order along the absorber. Titanium carbide material is more suitable in comparison with other coatings.

For the post boiling flow regime, known as super-heated flow, the simulation is accomplished similarly to ref. [1] other considered conditions are consistent with Tables 1, 2, 6. The pipe material is P-22 steel. By putting the obtained temperature profiles for the three different coatings in the present model, thermal stress analysis is performed. In Fig. 8 tangential stress distribution along the pipe obtained for the 3 different coatings can be seen. Temperature distribution for the outer surface of the pipe for different coatings is shown in Fig. 9.

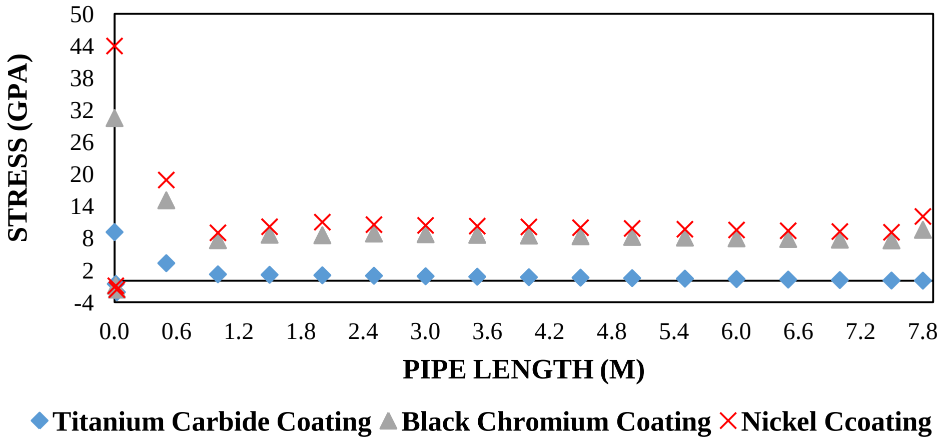

Fig. 8. Distribution of tangential stress along the absorber by synthetic oil fluid

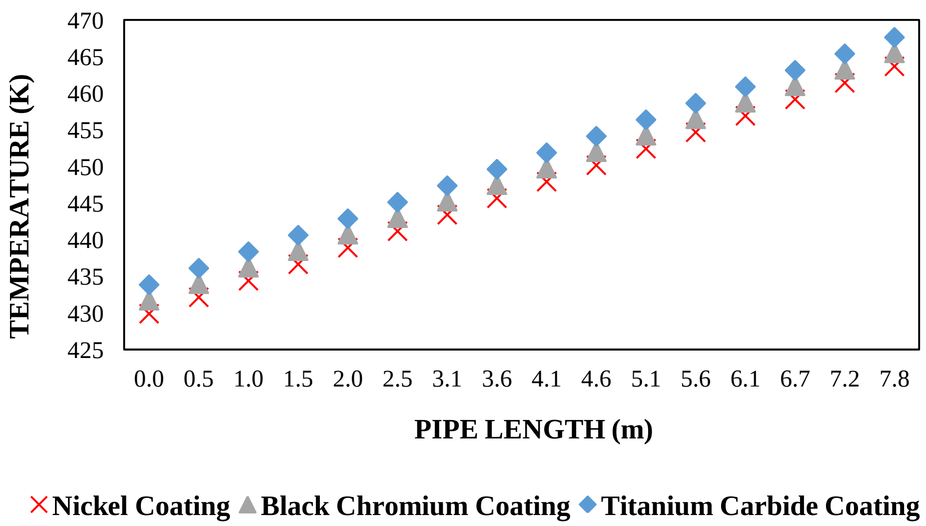

Fig. 9. Comparison of temperature distribution along the by synthetic oil

Then, by considering the mechanical properties in the stress simulation software for every three types of coating, the results of tangential stress by steam fluid along the absorber was obtained by analyzing, which the comparison of these three analyses can be seen in Fig.10. As well, for the present analysis, the results of Mises criterion was obtained too, which can be seen in Fig. 11. As seen in Fig. 10, tangential stress level along the absorber decreases respectively in the nickel, black chrome, and titanium carbide. As well it can be seen in the Mises stress distribution along the border which is cited in Fig. 11 and contains a higher precision.

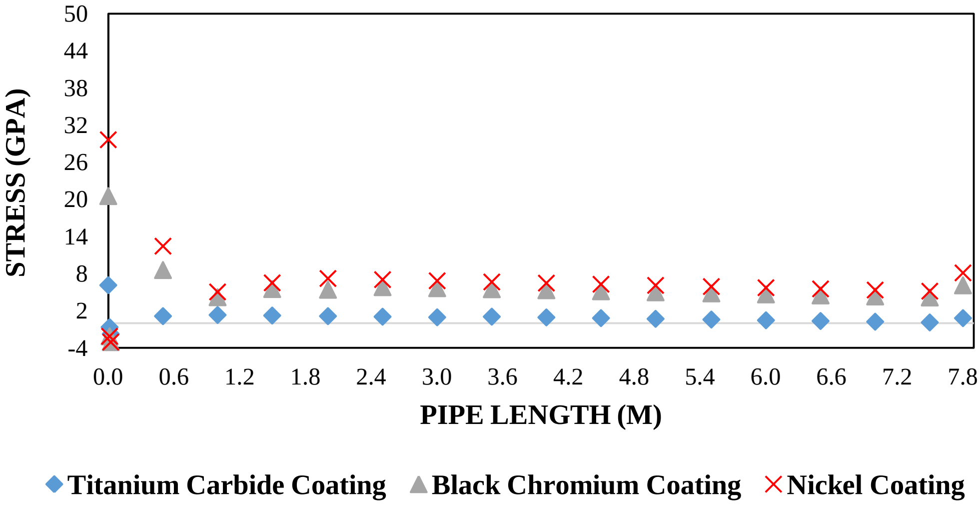

Fig. 10. Tangential stress comparison along the absorber at the superheating step by steam

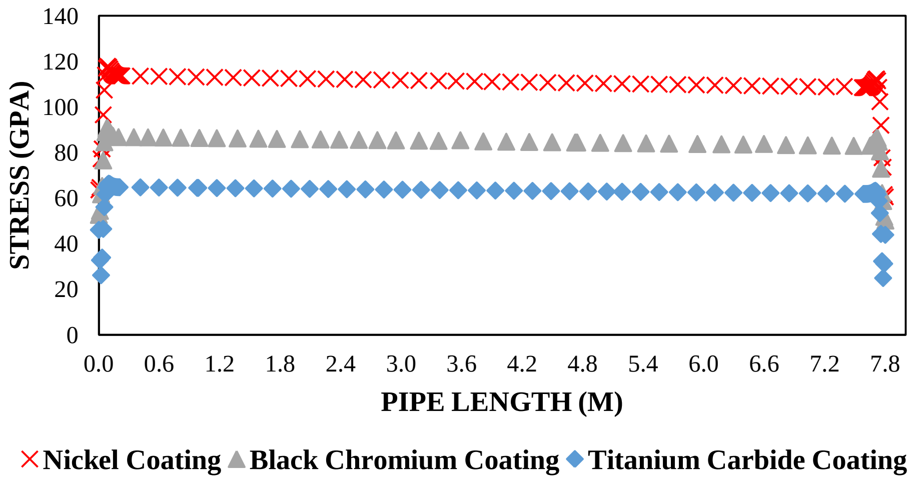

Fig. 11. Distribution of Mises stress at the superheating step by steam

13. Conclusion

Employing water as working fluid in direct steam generation systems is more welcomed due to environmental compatibility and inflammability in comparison with oils. Besides the mentioned advantages the probabilities of fractures due to thermal stresses exist by using water as the working fluids in absorbers. In the present study effects of applying different coating layers to improve the absorber properties and consequently to reduce thermal stresses are evaluated. In this regard, a comprehensive modeling from the single phase flow at the inlet of the absorber pipe to the superheated boiling flow at the outlet is accomplished to obtain temperature distribution and accordingly thermal stress all over the absorber surface. By the performed analysis it was concluded that a lower and uniform thermal stress distribution can be obtained by increasing thermal conductivity factor of the coated absorber.

It was found that by use of the boiling flow of water as the heat transfer fluid the level of stresses is 33% lower than the situation which the used fluid was synthetic oil. As the last concluding remark, the most optimized conditions for the absorber is using the titanium carbide coating with the pipe`s material of P-22 stainless steel.

Nomenclature

A_i - Internal area of absorber, [m^2]
C_p - Specific heat at constant pressure, [$Jkg^{-1}K^{-1}$]
Cr - Concentration factor
D_c - Diameter of mirror, [m]
$D_{g,ex\ or\ in}$ - External or Internal diameter of glass, [m]
$D_{a,\ ex\ or\ in}$ - External or Internal diameter of absorber, [m]
F_{rad} - Fraction of black body radiation in a wavelength band
g - Gravitational acceleration, [ms^{-2}]
I_{sun} - Radiation intensity of sun
k_g - Thermal conductivity for glass, [Wm-1K]
k_a - Thermal conductivity for absorber, [Wm-1K]
L - Length of absorber, [m]
$\dot{m}$ - Fluid flow rate, [kgs^{-1}]
Nu_c - Nusselt number for cavity
Pr - Prndtl number
Re - Reynolds number ($=\rho v D/\mu$)
Ra - Rayleigh number ($=g\beta(T_s\text{-}T_\infty)L^3/v\alpha$)
$T_{g,ex}$ - Temperature of external glass surface, [K]
$T_{g,in}$ - Temperature of internal glass surface, [K]
$T_{a,ex}$ - Temperature of external absorber surface, [K]
$T_{a,in}$ - Temperature of internal absorber surface, [K]
T_m - Fluid temperature at middle of absorber, [K]
T_i - Fluid temperature at input of absorber, [K]
T_o - Fluid temperature at output of absorber, [K]
T_{amb} - Ambient temperature, [K]
v - Fluid velocity, [ms^{-1}]
w - Wide of mirror, [m]
α_g - Absorptance coefficient of glass
α_a - Absorptance coefficient of absorber
β - Absorptance coefficient of mirror, [$1K^{-1}$]
β_c - Volumetric thermal expansion coefficient for cavity, [$1K^{-1}$]
β_g - Volumetric thermal expansion coefficient for glass, [$1K^{-1}$]
γ - Transmission coefficient ($=1\text{-}\alpha_g$)
ε_a - Emissivity coefficient for absorber
μ - Dynamic viscosity, [$kgs^{-1}m^{-1}$]
σ - Stefan – Boltzmann constant, [$Wm^{-2}K^{-4}$]
ρ - Fluid density, [kgm^{-3}]
Cr_g – Ratio between mirror focal and external diameter of glass ($=D_c/4D_{g,ex}$)
Cr_a - Ratio between mirror focal and external diameter of absorber ($=D_c/4D_{a,ex}$)

References

[1] A.A. Hachicha, I.Rodriquez, R. Capdevila, A. Oliva, Heat transfer analysis and numerical simulation of a parabolic trough solar collector, *Applied Energy* 111 (2013), pp. 581–592

[2] Hossein Tuysserkani, Principles of materials science (structure, properties and engineering), second edition, (2005)

[3] Huseyin Yapiji, Bilge Albayrak, Numerical solutions of conjugate heat transfer and thermal stresses in a circular pipe externally heated with non-uniform heat flux, *Energy Conversion and Management* 45 (2004), pp. 927–937

[4] Gulshah Ozishik, M. Serdar Gench, Huseyin Yapiji, Transient thermal stress distribution in a circular pipe heated externally with a periodically moving heat source, *International Journal of Pressure Vessels and Piping* 99-100 (2012), pp. 9-22

[5] A.A. Hachicha, I.Rodriquez, A. Oliva, Wind speed effect on the flow field and heat transfer around a parabolic trough solar collector, *Applied Energy* 130 (2014), pp. 200–211

[6] Fuqiang Wang, Yong Shuai, Yuan Yuan, Bin Liu, Effect of material selection on the thermal stresses of tube receiver under concentrated solar irradiation, *Materials and Design* 33 (2012), pp. 284–291

[7] Ricardo Vasquez Padilla, Gokmen Demirkaya, D. Yogi Goswami, Elias Stefanakos, Muhammad M. Rahman, Heat transfer analysis of parabolic trough solar receiver, *Applied Energy* 88 (2011), pp. 5097–5110

[8] David H. Lobon, Emilio Baglietto, Loreto Valenzuela, Eduardo Zarza, Modeling direct steam generation in solar collector with multiphase CFD, *Applied Energy* 113 (2014), pp. 1338-1348

[9] Naichia Yeh, Optical geometry approach for elliptical Fresnel lens design and chromatic aberration, *Solar Energy Materials & Solar Cells* 93 (2009), pp. 1309-1317

[10] M. Isabel Roldan, I. Canadas, J. L. Casas, E. Zarza, Thermal analysis and design of a solar prototype for high-temperature processes, *International Journal of Heat and Mass Transfer* 56 (2013), pp. 309-318

[11] Jafarkazemi, F., *et al.*, Energy and Exergy Efficiency of Heat Pipe evacuated tube solar collectors, *Thermal Science*, 20 (2016), 1, pp. 327-335

[12] Senthil, R., Cheralathan, M., Effect of non-uniform temperature distribution on surface absorption receiver in parabolic dish solar concentrator, *Thermal Science* (2015) doi: 10.2298/TSCI150609169S

[13] Yildizhan, H., Sivrioglu, M., Exergy analysis of a vacuum tube solar collector system having indirect working principle, Thermal Science, (2015), doi: 10.2298/TSCI150905009Y

[14] Vinod. S., *et al.*, Experimental and numerical analysis of convective heat losses from spherical cavity receiver of solar concentrator, *Thermal Science*. (2015) doi:10.2298/TSCI150601165S

[15] Zhu, *et al.*, Performance analysis of organic Rankine cycles using different working fluids, *Thermal Science, 19* (2015), 1, pp. 179-191

[16] Ze-Dong Cheng, Ya-Ling He, Kun Wang, Bao-Cun Du, F.Q. Cui, A detailed parameter study on the comprehensive characteristics and performance of a parabolic trough solar collector system, *Applied Thermal Engineering* 63 (2014), pp. 278-289

[17] S. M. Akbarimoosavi, M. Yaghoubi, 3D Thermal-structural analysis of an absorber tube of a parabolic trough collector and the effect of tube deflection on optical efficiency, *Energy Procedia* 49 (2014), pp. 2433 – 2443

[18] Frank P. Incropera, David P. Dewitt, *Fundamentals of Heat and Mass Transfer*, John Wiley & Sons Inc., New York, USA, seven edition, 2007

[19] Iyad Al-Zaharnah, Thermal Stresses in Pipes, Ph.D. Thesis, School of Mechanical & Manufacturing Engineering, Dublin City University, Dublin, Republic of Ireland, April 2002

[20] David H. Lobon, Emilio Baglietto, Loreto Valenzuela, Eduardo Zarza, Modeling direct steam generation in solar collectors with multiphase CFD, *Applied Energy* 113 (2014), pp. 1338–1348